Available online at www.sciencedirect.com
SCIENCE DIRECT®
Optics Communications 238 (2004) 335–340
OPTICS COMMUNICATIONS
www.elsevier.com/locate/optcom

Bessel–Gauss output beam from a diode-pumped Nd:YAG laser

A. Hakola [a,*], S.C. Buchter [a], T. Kajava [a], H. Elfström [b], J. Simonen [b]
P. Pääkkönen [b], J. Turunen [b]

[a] *Department of Engineering Physics and Mathematics, Helsinki University of Technology, P.O. Box 2200, FI-02015 HUT, Finland*
[b] *Department of Physics, University of Joensuu, P.O. Box 111, FI-80101 Joensuu, Finland*

Received 3 February 2004; received in revised form 6 April 2004; accepted 6 May 2004

Abstract

We demonstrate a simple and compact laser source that directly produces a Bessel–Gauss beam. The laser resonator consists of a diode-end-pumped Nd:YAG crystal, a planar mirror, and a diffractive mirror designed to phase-conjugate only the lowest-order Bessel–Gauss beam.

PACS: 42.55.Xi; 42.60.Jf; 42.25.Fx
Keywords: Bessel–Gauss beam; Propagation invariant; Diffractive mirror; Diode-pumped laser

1. Introduction

Bessel–Gauss beams [1] form an interesting class of physically realizable approximations of the propagation-invariant Bessel fields [2–4]. Due to the Gaussian apodization of the ideal Bessel amplitude distribution, the beam retains its diffraction-free properties only within a finite range but its propagation can be described everywhere by rather simple analytical formulae.

Bessel–Gauss beams find applications, e.g., in precision alignment [5] and in guiding and confining charged particles or neutral atoms [6,7]. Because of their intriguing properties and potential applications, several ways to realize Bessel fields have been proposed and demonstrated. Most of them are based on a laser source and a separate passive optical element or system such as an axicon [8,9], a ring aperture together with a positive lens [2,3], a Fabry–Perot interferometer [10,11], or a two-element diffractive system [12]. Schemes to produce Bessel-type modes in laser resonators have also been proposed [13–19], but only a few experiments of such active sources have been

* Corresponding author. Tel.: +358-9-4513165; fax: +358-9-4513195.
E-mail address: antti.hakola@hut.fi (A. Hakola).

0030-4018/$ - see front matter
doi:10.1016/j.optcom.2004.05.012

reported: An argon-ion laser with an annular end mirror and a positive intracavity lens that produced an approximation of the fundamental Bessel beam [20] and a laser resonator with two plane mirrors and an axicon placed close to one of them [17]. In addition, some optically pumped vertical-cavity laser resonators with circular distributed feedback mirrors have produced azimuthally polarized fields of the Bessel–Gauss type [21].

Recently, there has been much interest in the use of aspheric-mirror resonators [22] to produce various types of non-Gaussian laser beams [23] including approximate Bessel fields [24]. Here, we apply these ideas and demonstrate an active source for Bessel–Gauss beams. The design is based on a compact solid-state laser, end-pumped with a diode laser. The concave output coupler of the plano-concave resonator is replaced with a diffractive mirror designed to conjugate the phase of only the lowest-order Bessel–Gauss mode. In this way, we obtain an output beam whose intensity distribution and propagation characteristics are in good agreement with theory. In earlier resonator designs to produce Bessel–Gauss beams with the help of axicons [17], the propagation-invariant distance has to be smaller than the cavity length. This is a consequence of the fact that the field at the axicon should essentially be the far field. On the contrary, there is no such limit in our method: the distance can in principle be freely changed by using elements with different design parameters. Thus, the cavity length can be only a small fraction of the propagation-invariant range of the Bessel–Gauss beam.

2. Bessel–Gauss beams

The field distribution at the waist of an mth-order Bessel–Gauss beam is given by

$$U(\rho, z=0, \phi) = J_m(\alpha\rho)\exp\left(-\rho^2/w_0^2\right)\exp\left(\mathrm{i}m\phi\right), \tag{1}$$

where α and w_0 are constants, ρ is the radial distance from the optical axis of the beam, and J_m is the Bessel function of the first kind and mth order. From Eq. (1) it is easy to see that when $w_0 \to \infty$ the distribution approaches a Bessel function, while the case $\alpha = m = 0$ represents a pure Gaussian function. In this sense, Bessel–Gauss beams can be considered as a smooth transition from the propagation-invariant Bessel fields to Gaussian laser beams.

Upon propagation, the Bessel–Gauss beam diverges and acquires wavefront curvature, forming a ring-shaped far-field pattern [1]. In order to gain understanding on the properties of such a beam, one may imagine that it is formed as a superposition of Gaussian beams whose axes lie on a cone (around the z-axis) with a half angle θ defined by $\sin\theta = \alpha/k$, where k is the wave number. The propagation characteristics of the beam are thereby governed by the spreading of the beam due to the conical propagation and the diffraction of the Gaussian beams (diffraction angle $\theta_G = 2/(w_0 k)$). When $\theta \ll \theta_G$, the whole beam behaves like a Gaussian beam, whereas the case $\theta \gg \theta_G$ represents a Bessel-like beam with a propagation-invariant range of approximately $L_0 = w_0/\theta$. At this distance, according to approximate geometrical optics arguments, the Gaussian beam components have moved a radial distance of w_0 from the z-axis so that an annular beam starts to form. Mathematical representation for the the Bessel–Gauss field at a distance z is obtained by substituting Eq. (1) into the Fresnel propagation formula, which yields

$$\begin{aligned} U(\rho, z, \phi) = {} & \frac{w_0}{w(z)}\exp[\mathrm{i}\Phi(z)]J_m\left(\frac{\alpha\rho}{1+\mathrm{i}z/z_R}\right) \\ & \times \exp\left\{-\left[\frac{1}{w^2(z)} - \frac{\mathrm{i}k}{2R(z)}\right](\rho^2 + \theta^2 z^2)\right\} \\ & \times \exp(\mathrm{i}m\phi), \end{aligned} \tag{2}$$

where $k = 2\pi/\lambda$ and z_R is the Rayleigh range. The propagation laws for the spot size $w(z)$ and the wavefront curvature $R(z)$ are the same as for Gaussian beams. In addition, $\Phi(z) = \beta z - \arctan(z/z_R)$, where $\beta = k - \alpha^2/2k$, is the axial phase of the beam. One thus notices that the propagation of a Bessel distribution gives rise to distinct aspheric phase factors, which can be utilized in mode discrimination within laser resonators.

3. Design of the Bessel–Gauss laser

A schematic illustration of the Bessel–Gauss laser is shown in Fig. 1. A 5 mm long and 3 mm diameter, 1% Nd-doped YAG rod is pumped with a

2 W diode laser (JDS Uniphase 2462) at 808 nm. The FWHM divergences of the diode-laser beam are $\theta_{\parallel} = 12°$ and $\theta_{\perp} = 32°$ in the directions parallel and perpendicular to the diode junction, respectively. This beam is collimated and focused to an approximately 100 μm spot in the YAG crystal. The end face of the YAG crystal is coated to provide high reflectivity for the laser wavelength of 1064 nm and high transmissivity for the 808 nm pump beam. The drive current of the diode laser was limited to 2 A, which corresponded to a maximum pump power of 1.3 W. Approximately 95% of this power was absorbed in the YAG crystal.

The resonator is a simple linear cavity, where the concave end mirror is replaced by a diffractive mirror with the surface profile also shown in Fig. 1. The 2.7 mm diameter structure was patterned in a 1-inch fused-silica substrate using electron beam lithography and proportional reactive ion etching [25,27]. A nearly analog depth profile was obtained using 32 depth levels when exposing the element. The average depth of the element was 543 nm, which means an approximately 2% error from the goal depth of 532 nm. Finally, we sputtered a 5 nm layer of chromium for adhesion and a 130 nm layer of gold on the element. The measured reflectivity of this coating was greater than 99% at 1064 nm. In an 8 cm resonator, this particular element was designed to support the zeroth-order Bessel–Gauss mode with a 300 μm waist at the YAG crystal. Combining this with the design value for the cone angle, 3.75 mrad, the propagation-invariant distance also becomes $L_0 = 8$ cm. This particular value was selected based on Fox–Li simulations such that the resulting mode would be a compromise between a long Bessel–Gauss beam and the number of intensity rings – the longer the distance L_0, the more the field resembles a Gaussian beam. Note that the propagation-invariant distance can be easily adjusted to any value with a telescope [26]. Shortening the cavity length from 8 cm down to 3 cm did not have substantial effects on the intensity profile of the output beam, which is an indication of the propagation-invariant properties of the Bessel–Gauss beam within this range. This fact was also verified by Fox–Li simulations. A 3 mm thick uncoated fused-silica plate at an angle close to Brewster's angle was placed in the resonator to couple out a small part of the intracavity beam. A small wedge in the plate provided a spatial separation of the reflections from the two surfaces. This arrangement permitted imaging of the beam profile both inside and outside of the resonator onto a CCD camera.

4. Experimental results

With the arrangement of Fig. 1, without the wedge plate, we obtained laser operation at an absorbed pump power of 265 mW. We also measured fundamental mode thresholds for cavities with spherical mirrors (reflectivities 94%, 98%, and 99.9%) producing approximately the same mode size in the YAG crystal as the diffractive element. We then performed a traditional Findlay–Clay

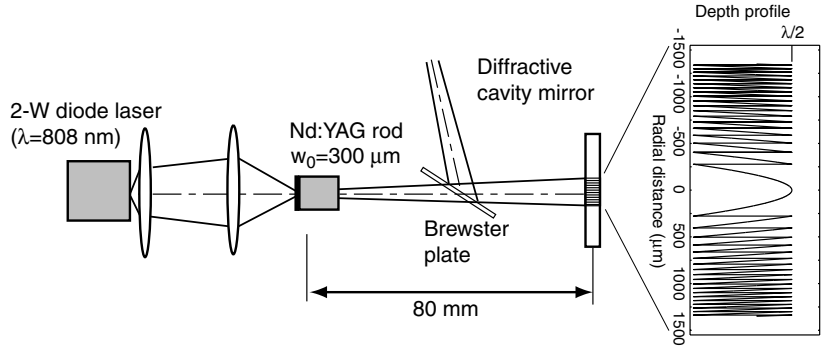

Fig. 1. Schematic illustration of the Nd:YAG laser cavity designed to produce Bessel–Gauss beams.

analysis [28] and determined the additional loss introduced by the element to be approximately 5%. This loss is presumably due to fabrication errors resulting in a reduced diffraction efficiency. The fundamental Bessel–Gauss beam was also produced in a cavity, where the YAG rod was re-

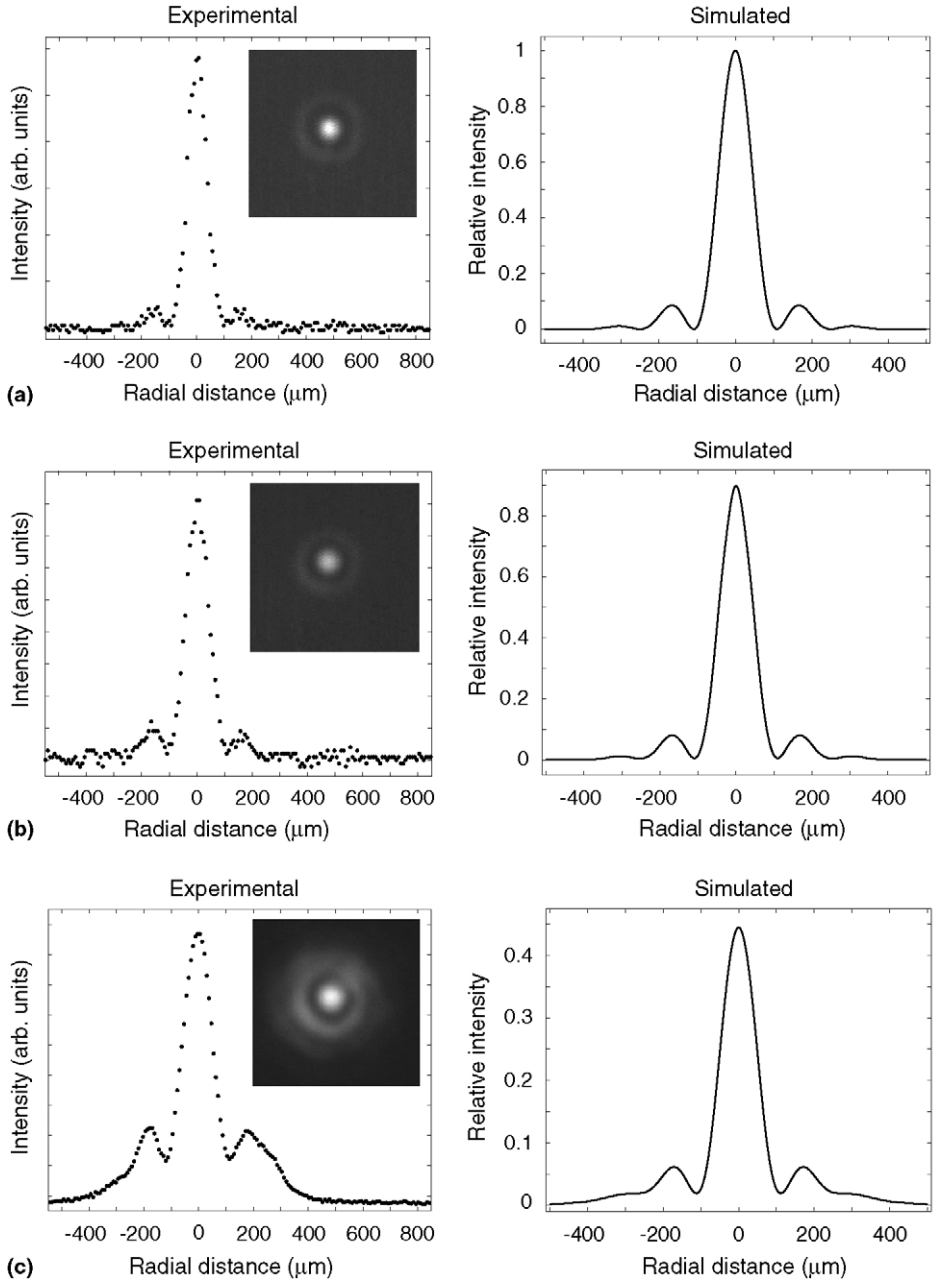

Fig. 2. Measured radial intensity profiles together with CCD images (left column) and theoretical profiles (right column) of the Bessel–Gauss beam measured at locations corresponding to distances of (a) 0, (b) 2 and (c) 5 cm from the beam waist. The scale in the theoretical curves is directly obtained from Eq. (2) when the intensity of the central peak at the beam waist is normalized to unity.

placed by a 2% Nd-doped YVO_4 crystal (dimensions $3\times3\times1.2$ mm^3). In that case, the threshold pump power was approximately two times lower than with YAG.

Two-dimensional images of the beam measured at locations corresponding to distances of 0, 2 and 5 cm from the beam waist are shown in Fig. 2. This figure also presents radial intensity distributions of the beam together with theoretical profiles calculated from Eq. (2) at the same distances. These images show that the measured and the theoretical intensity profiles match well with each other. The first minimum is reached at slightly above 100 μm, which is in agreement with the theoretical value of 108.6 μm. The intensity ratio of the first and the secondary maxima in the measured profiles also behaves similarly to the theoretical curves as the beam propagates. In addition, profile measurements at other locations within the designed propagation-invariant range correspond well with the theoretical curves obtained from Eq. (2). The beam is slightly asymmetric, most probably due to aberrations caused by small radial and azimuthal depth errors in the profile of the diffractive mirror. The radially varying feature size, for instance, gives rise to spherical aberrations. In addition, even a small misalignment of the laser resonator had a noticeable effect on the beam behavior, particularly in the far field. Due to these effects, the secondary maxima in Fig. 2 appear higher than what one would expect theoretically; this behavior can be clearly seen in the profile measured at 5 cm from the waist. Numerical simulations, on the other hand, show that the main effect of a constant error in the goal depth are increased losses, whereas the beam shape remains essentially the same. For example, a 10% depth error produces an intracavity loss, which corresponds to an almost 20% decrease in the beam intensity.

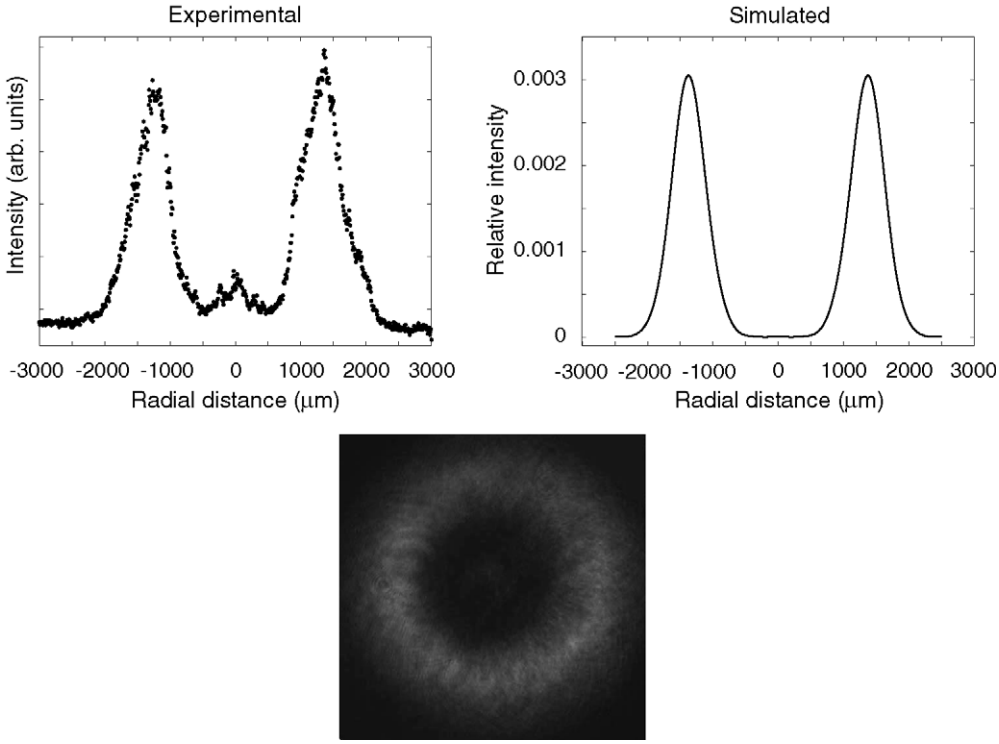

Fig. 3. Experimental and theoretical intensity profiles (top row) and CCD image (bottom row) of the Bessel–Gauss beam in the far field (distance 38 cm from the waist). The vertical scale in the theoretical profile is the same as that in Fig. 2.

The one- and two-dimensional intensity distributions of the Bessel–Gauss beam in the far field are shown in Fig. 3. The images are taken at the distance of 38 cm from the waist. As expected, the profile has transformed to a ring with a peak-to-peak diameter of approximately 2.5 mm. Moreover, only faint traces of the zeroth-order peak can be seen around the center point of the measured profile. The most probable origin of this zeroth-order component are small errors in the element depth profile. From Fig. 3, we estimate the cone angle to be $\theta \approx 1.28$ mm/380 mm = 3.4 mrad, which is somewhat smaller than the estimate obtained from the theoretical profile ($\theta = 3.6$ mrad). Based on Figs. 2 and 3, we conclude that the beam produced in the resonator is indeed a fundamental Bessel–Gauss beam.

5. Conclusions

We have demonstrated a compact, diode-pumped Nd:YAG laser that is based on a diffractive resonator mirror and that operates in the fundamental Bessel–Gauss mode. Unlike most other approaches, this technique allows the generation of the exact Bessel–Gauss beam with a practical limit given only by the accuracy at which the element can be fabricated. This is not a serious limitation since the structure sizes are rather large (tens of micrometers) and the element itself is small. We observed a slight beam distortion and determined an approximately 5% intracavity loss attributed to fabrication errors of this particular element. Better elements are clearly possible but already this quality is sufficient to produce output powers and efficiencies typical for compact diode-pumped solid-state lasers. This is therefore an attractive way to produce Bessel–Gauss as well as other non-Gaussian beams directly from a laser source.

Acknowledgement

The work of Henna Elfström and Antti Hakola was supported by the Ministry of Education, Finland, under the Graduate School on Modern Optics and Photonics.

References

[1] F. Gori, G. Guattari, C. Padovani, Opt. Commun. 64 (1987) 491.
[2] J. Durnin, J. Opt. Soc. Am. A 4 (1987) 651.
[3] J. Durnin, J.J. Miceli Jr., J.H. Eberly, Phys. Rev. Lett. 58 (1987) 1499.
[4] It should be noted that several properties of Bessel and Bessel–Gauss fields were predicted long before they became a subject of widespread interest; see C.J.R. Sheppard, T. Wilson, Microwaves, Opt. Acoust. 2 (1978) 105 where generation of Bessel–Gauss beams in toroidal resonators is also discussed.
[5] G. Bickel, G. Häusler, M. Maul, Opt. Eng. 24 (1985) 975.
[6] M. Florjanczyk, R. Tremblay, Opt. Commun. 73 (1989) 448.
[7] J. Arlt, T. Hitomi, K. Dholakia, Appl. Phys. B 71 (2000) 549.
[8] J.H. McLeod, J. Opt. Soc. Am. 44 (1954) 592.
[9] J.H. McLeod, J. Opt. Soc. Am. 50 (1960) 166.
[10] J. Turunen, A. Vasara, A.T. Friberg, Appl. Opt. 27 (1988) 3959.
[11] A.J. Cox, D.C. Dibble, J. Opt. Soc. Am. A 9 (1992) 282.
[12] P. Pääkkönen, J. Simonen, M. Honkanen, J. Turunen, J. Mod. Opt. 49 (2002) 1943.
[13] J. Durnin, J.H. Eberly, US Patent 4,887,885 (1989).
[14] J.K. Jabczyński, Opt. Commun. 77 (1990) 292.
[15] P. Muys, E. Vandamme, Appl. Opt. 41 (2002) 6375.
[16] J. Rogel-Salazar, G.H.C. New, S. Chávez-Cerda, Opt. Commun. 190 (2001) 117.
[17] A.N. Khilo, E.G. Katranji, A.A. Ryzhevich, J. Opt. Soc. Am. A 18 (2001) 1986.
[18] J.C. Gutiérrez-Vega, R. Rodríguez-Masegosa, S. Chávez-Cerda, J. Opt. Soc. Am. A 20 (2003) 2113.
[19] N. Chattrapiban, E.A. Rogers, D. Cofield, W.T. Hill III, R. Roy, Opt. Lett. 28 (2003) 2183.
[20] K. Uehara, H. Kikuchi, Appl. Phys. B 48 (1989) 125.
[21] T. Erdogan, O. King, G.W. Wicks, D.G. Hall, E. Anderson, M.J. Rooks, Appl. Phys. Lett. 60 (1992) 1921.
[22] P.A. Bélanger, C. Paré, Opt. Lett. 16 (1991) 1057.
[23] J.R. Leger, D. Chen, Z. Wang, Opt. Lett. 19 (1994) 108.
[24] P. Pääkkönen, J. Turunen, Opt. Commun. 156 (1998) 359.
[25] P. Laakkonen, High-efficiency diffractive optics with electron beam lithography, Ph.D. Thesis, University of Joensuu, Joensuu, 2000.
[26] M. Santarsiero, Opt. Commun. 132 (1996) 1.
[27] P. Laakkonen, J. Lautanen, V. Kettunen, J. Turunen, M. Schirmer, J. Mod. Opt. 46 (1999) 1295.
[28] D. Findlay, R.A. Clay, Phys. Lett. 20 (1966) 277.